Shear Microscopy of the "Butterfly Pattern" in Polymer Mixtures

Elisha Moses,* Takuji Kume, and Takeji Hashimoto
Department of Polymer Chemistry, Kyoto University, Kyoto 606, Japan
(Received 1 July 1993)

The concentration fluctuations induced in a semidilute polymer solution by shear flow are directly visualized for the first time. The spatial structure of the "butterfly pattern" observed by light scattering is elucidated, being the result of hydrodynamic rippling waves which have a distribution of tilt angles. The minimal tilt angle depends on shear rate in a power law fashion, causing the butterfly to almost close upon itself at high shear rates. The concentration waves have a time scale related to a shear rate $\dot{\gamma} \sim 1$ sec^{-1} and periodicity $\lambda \sim 10$ μm, indicating a link to reptation processes.

PACS numbers: 61.25.Hq, 47.50.+d, 83.50.Ax

Shear induced phase separation is one of the striking results of combining hydrodynamics with the special elastic and viscous properties of polymers, and has been the center of a concentrated effort in recent years [1–10]. It originates in the profound effects of entanglement and coil stretching upon the flow of semidilute, high molecular weight polymer solution. While our notion of mixing by shear flow is intuitively consistent with shear induced homogenization in lower molecular weight systems [11], the appearance of systems where shear induces phase separation was quite remarkable. When shear induced separation was first observed experimentally [1,2], it was attributed to an elastic term in the free energy [2]. Such a contribution could move the critical curve sufficiently to allow phase separation at elevated temperatures. More recently, Helfand and Frederickson (HF) suggested [3] that this separation is not a thermodynamic phase transition, but rather a nonequilibrium result of the coupling between the stress field and the polymer concentration field.

A first clue to the hydrodynamic origin of the separation can be found in light scattering experiments, which showed a strong anisotropy of the scattering pattern with respect to the flow direction [6,8]. In these experiments the salient feature is the "butterfly pattern" obtained from small-angle light scattering (SALS). It is characterized by a dark streak in the direction perpendicular to the flow, where there is no enhancement of the scattering. In the direction of the flow a strong enhancement of the scattering occurs that is limited in width to an opening angle 2α which increases with shear rate. Such anisotropy would not occur if the transition were a thermodynamic phase transition. A qualitative confirmation of the HF theory was given in a Couette flow light scattering experiment [7], where the experimental axes of the scattering rays were made to correspond to those in the calculation of HF. In this paper we present the first direct observation and visualization of the actual participating hydrodynamic modes.

The butterfly pattern has also been observed in other polymer systems, and is attracting much attention [12–17]. It has shown up in stretched rubber, polymer gels, and polymer melts. There it is found at much smaller wavelengths, by use of neutron scattering. It is worth noting that the butterfly pattern was also reported for stretched block copolymer films containing spherical microdomains of polystyrene in the rubbery matrix of polyisoprene [18]. A feature universal to the butterfly pattern is that spatial heterogeneities (concentration fluctuations of polymer molecules or centers of spherical domains) are built up in the direction of the applied fields, while the heterogeneities remain essentially unaltered in the direction perpendicular to the fields.

To elucidate the structure which yields the butterfly pattern, we introduced a new measurement into our system, a flow visualization that could be operated in conjunction with the SALS. This enabled a direct measurement of the concentration fluctuations through their effect on the index of refraction. We then used computer enhanced video techniques [19] to identify the participating hydrodynamic modes. We have found that the butterfly pattern is the effect of waves, or ripples, that are tilted at varying angles β with respect to the flow direction, but are limited by a minimal angle β_m which decreases with the shear rate.

Our experimental setup is a modified version of the one described in Ref. [6]. We used a cone and plate rheometer with glass components made out of quartz (the cone angle used was 2.6°). The cone and plate are encased in a temperature regulated volume, with long term stability of ± 0.1 K. Apertures in the temperature enclosure (~ 1 cm diam) allow illumination from below and the insertion of a modified Nikon microscope from above (we used white light and Nikon 10×, 20×, and 60×, $a = 6$ mm objectives). For scattering measurements the microscope was removed, HeNe laser light used, and a photographic film placed ~ 30 cm above the plate. The polymer solution is sheared between the fixed top plate and the rotating cone below, in a gap which goes continuously from ~ 100 μm to ~ 3 mm. The conical wedge ensures a constant shear rate so long as the flow is a simple shear. For the visualization we used a fast shutter (1/10000 sec) charge-coupled-device video camera (Sony SSC-M370) connected in parallel to a Macintosh IIci with frame

0031-9007/94/72(13)/2037(4)$06.00

grabber (RasterOps 24STV) and to a SVHS VCR (Victor HR-S6600). For technical reasons the shutter limits the use to single fields, decreasing the effective spatial resolution by half.

In a shear flow we distinguish between a flow direction (z axis) along which the velocity is constant, a direction in which the dominant, shearing flow velocity gradient exists (x axis) and a neutral direction (y axis). In our cone and plate experiment the dominant velocity gradient lies in the vertical gap between the (fixed) top plate and the (rotating) cone. The incident light beams that we use for visualization or for scattering enter through the transparent cone at the bottom of the apparatus, traverse the sample along the x axis, and exit the cell through the transparent top. The data are recoded above the cell, onto a screen (for light scattering) or into the microscope (for visualization). Thus we view the y-z plane which contains the flow (tangential) and neutral (radial) directions. Note that HF treat the x-z plane, which is also the one visualized in Ref. [7].

We used polystyrene with weight average molecular weight M_W of 5.48×10^6 and heterogeneity index $M_W/M_n=1.15$, where M_n is the number average molecular weight, dissolved at 6.0 wt.% in dioctylphtalate (DOP), a θ solvent at 22°C. This concentration is about 40 times the overlap concentration c^*. The cloud point was at 13.8°C, and we worked in the one phase region at 27°C.

Figure 1 shows the butterfly pattern as observed by SALS for three of our shear rates. For reference we also present the signal at no shear, where the only signal comes from the direct beam, and no scattering is apparent. This indicates that prior to shearing the solution is indeed in the homogeneous, one phase region. Once the shear rate is strong enough, a characteristic anisotropic pattern appears, whose dominant feature is the dark streak perpendicular to the flow direction. In the direction of the flow there is enhanced scattering, indicative of a structure with periodicity in the flow direction and extent in the direction perpendicular to the flow. This enhancement extends out to the "butterfly wings," indicating that the periodicity exists at the distribution of angles with respect to the flow direction. As the shear rate increases, the "wings" spread and invade into the dark streak, which almost disappears for the high shear rate.

The microscope visualization of the structures in the flow is presented in Fig. 2. Again the zero shear picture emphasizes the appearance of a structure as the shear is applied. A signal can be discerned already at a shear rate $\dot\gamma$ of 0.116 $\sec^{-1}$, and at 0.231 $\sec^{-1}$ we see clearly the appearance of a periodic structure with a length scale of approximately 10 μm. These ripples were observed at low shear rates to form and disappear on a time scale of $\sim$1 sec, and their lateral extent is much longer than the periodicity. At the lower shear rates the waves are mostly oriented perpendicular to the flow. As the shear rate increases, the waves tilt with respect to the direction of the flow. The smallest accessible angle $\beta_m(\dot\gamma)$ decreases, until the shear rate of 16.2 $\sec^{-1}$ at which the waves can

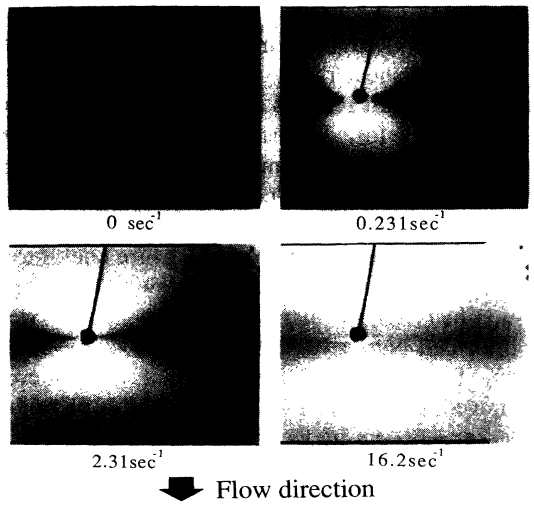

FIG. 1. SALS patterns show the appearance and development of the butterfly pattern. Photographs taken at 1/250 sec shutter speed, except for 0 $\sec^{-1}$, taken at 1/30 sec. The halo around the beam stop at 0 $\sec^{-1}$ gives an indication of the parasitic scattering.

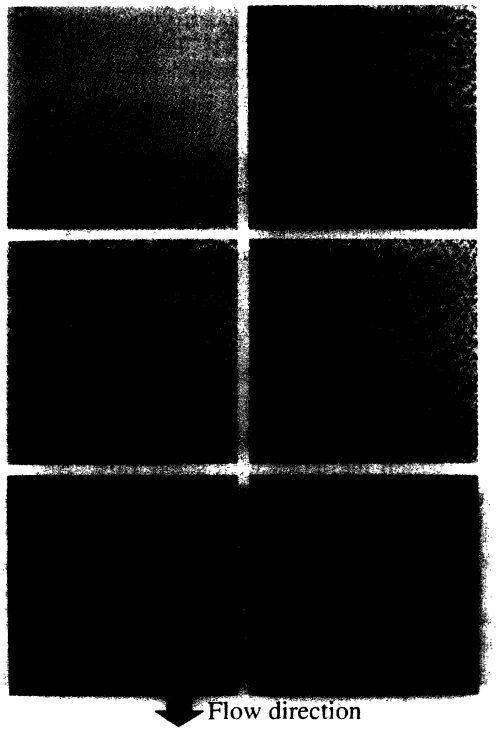

FIG. 2. Microscope visualization images of the concentration fluctuations. Numbers indicate shear rate in $\sec^{-1}$.

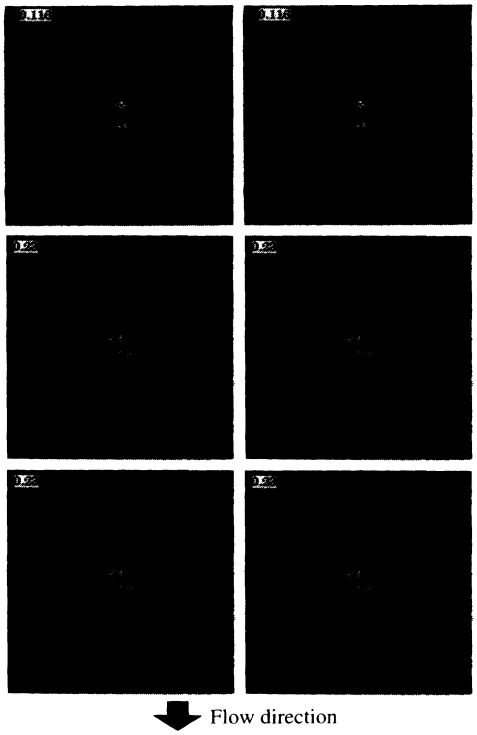

FIG. 3. FFT spectra of the images as in Fig. 2.

be almost parallel with the flow ($\beta_m \cong 20°$).

To ascertain that the visualization pictures are a true representation in real space of the butterfly pattern we take the fast Fourier transform (FFT) of the patterns. The spectra corresponding to the pictures of Fig. 2 are presented in Fig. 3. To reconstruct the light scattering representation of k space of Fig. 1 we use in Fig. 3 a logarithmic gray scale representation with constant contrast enhancement. The similarity of the Fourier spectra with the signal obtained by light scattering is apparent.

These pictures constitute our spatial explanation for the appearance of the butterfly pattern: The dark streak perpendicular to the flow (in the y direction) in the SALS pattern arises because there is no periodicity (no concentration fluctuations) in that direction (the solution remains homogeneous in that direction). Waves that are perpendicular to the flow direction contribute a scattering intensity parallel to the flow (z direction), while those waves that are oriented in the range of allowed angles fill up the "wings" of the pattern, up to a maximal angle determined by $\alpha_m(\dot\gamma)$, with the connection to the (minimal) spatial angle given by $\alpha_m = 90° - \beta_m$. Beyond α_m no periodicity exists and the dark streak begins.

The periodicity of ~ 10 μm observed in the pictures is consistent with a peak in the SALS pattern at a similar wavelength (~ 9.3 μm) [8] that shows up at high shear rates. We applied a bandpass filter centered around $\lambda = 9$ μm by digital convolution, followed by binary thresholding of the filtered signal to enhance the contrast. The results of this process are presented in Fig. 4, spanning over two decades in shear rate.

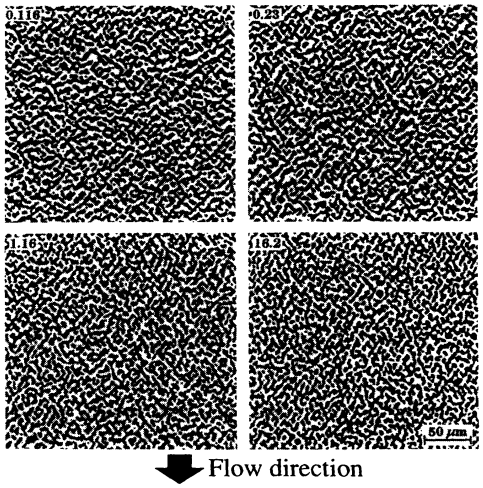

FIG. 4. Microscope images after bandpass convolution and thresholding. Numbers indicate shear rate in $\sec^{-1}$.

Close inspection of the filtered data shows the distribution of waves at different angles. The waves of largest lateral extension have similar orientation, at $\pm\beta_m(\dot\gamma)$ with respect to the flow direction. The lateral extent of the waves can go from as short as 20–30 μm up to a few hundred μm, which is our whole field of view. Waves with high angles exist, up to 90° with respect to the flow, but their extent is short.

To evaluate the angular distribution of the waves we skeletonized the figures, keeping the edges of the resulting graph as relevant segments. This caused a loss of long range correlations, but the angular dependence is still strong. To reduce high frequency noise segments shorter than the wavelength of ~ 9 μm were discarded, and on the remaining segments angles were computed. To eliminate scatter originating in the pixel matrix, we discarded short distances, then renormalized by an isotropic distribution, and applied data smoothing. The resulting distributions are presented in Fig. 5. Since there was no apparent asymmetry in the plus or minus β distribution, we plot the modulus of the angle.

We identify the angle at which the peak in the angular distributions begins (or shoulder for $\dot\gamma = 0.116$ $\sec^{-1}$) with $\beta_m(\dot\gamma)$. The inset to Fig. 5 shows the trend of a power law over the two decades spanned, with $\beta_m \to 0$ as $\dot\gamma \to \infty$. Approaching the limit, however, is impractical, due to the appearance at $\dot\gamma \geq \dot\gamma_a \cong 7$ $\sec^{-1}$ of a rheological anomaly [8]. As a guide to the eye we give a best fit to a power law $\beta_m = 0.5\dot\gamma^{-1/7}$, with β_m in radians and $\dot\gamma$ in $\sec^{-1}$.

The origin of the wavelength (and the length scale observed by SALS at $\dot\gamma \geq \dot\gamma_a$) is an interesting question. One explanation is that a reptation process is dominating the hydrodynamic structures we observe [20]. The time

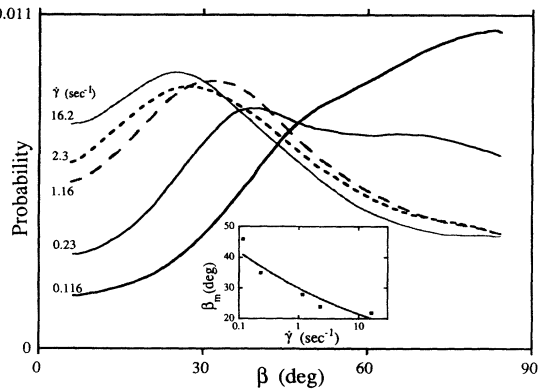

FIG. 5. Normalized probability histograms of the angular distribution of segments from skeletonized microscope images for various shear rates. Flow direction is at 0°. Inset: Shear rate dependence of the minimal angle β_m. Solid line is the fit to a power law.

scale for reptation τ_{rep} of our polymers is on the order of 1–10 sec. The argument (based on the work of Brochard and de Gennes [21]) is that in the absence of shear fluctuations decay by cooperative diffusion (with coefficient [7] $D_{fluid} \sim 10^{-6}$ cm^2/sec). In the presence of shear the flow of solvent into polymer-rich regions produces a transient elastic deformation which reduces the thermodynamic force driving the solution to equilibrium, and effectively arrests the relaxation of a density fluctuation. The transient stress decays after a typical relaxation time determined by reptation, τ_{rep}. This defines a viscoelastic length scale $\lambda = (D_{fluid}\tau_{rep})^{1/2}$ on which the slowing down of the decay of fluctuations is most pronounced, i.e., on which fluctuations are enhanced [22]. We thus obtain $\lambda \cong 10$–30 μm, close to the length scale we measure (a similar argument in Ref. [7] yielded ~ 1 μm for that system).

Note that the rotation of the scattering pattern with increasing shear rate described by HF and observed in Ref. [7] occurs in the x-z plane, while we report rotation of the spatial pattern with increasing shear rate in the y-z plane. Three-dimensional effects are clearly important, and should be taken into consideration in any theoretical treatment which would endeavor to explain the waves and their tendency to tilt.

In summary, we have demonstrated that the spatial origin of the butterfly pattern in shear flow of semidilute, high molecular weight polymer solutions is the existence of hydrodynamic modes, or ripples, which have a distribution of tilt angles. The FFT of the patterns obtained by shear microscopy reproduces well the light scattering pattern. There exists a minimal angle β_m with respect to the flow, beyond which no wave can tilt. This causes a dark streak with angle $2\beta_m = 180° - 2\alpha_m(\dot{\gamma})$, in the direction perpendicular to the flow, which is the salient characteristic of the butterfly pattern. β_m tends to 0° at high shear rates, causing the butterfly to almost close upon itself. The wavelength of the waves is ~ 10 μm, and a time scale which arises from viewing the lifetime of the ripples, from a peak in the scattering intensity, from rheological measurements [7], from the rotation of the scattering pattern [7], and from an argument about reptation is $\tau_{rep} = 1$ sec, or $\dot{\gamma} = 1$ sec^{-1}.

We thank A. Onuki, Y. Rabin, and T. Witten for fruitful discussions and insight. E.M. acknowledges the support of a JSPS fellowship.

*Present address: Weizmann Institute of Science, Physics Department, Rehovot 76100, Israel.

[1] G. Ver Strate and W. Phillipoff, J. Polym. Sci. Polym. Lett. **12**, 267 (1974).
[2] C. Rangel-Nafaile, A. B. Metzner, and K. F. Wissbrun, Macromolecules **17**, 1187 (1984).
[3] E. Helfand and G. H. Fredrickson, Phys. Rev. Lett. **62**, 2468 (1989).
[4] A. Onuki, Phys. Rev. Lett. **62**, 2472 (1989); J. Phys. Soc. Jpn. **59**, 3424 (1990).
[5] S. T. Milner, Phys. Rev. Lett. **66**, 1477 (1991).
[6] T. Hashimoto and K. Fujioka, J. Phys. Soc. Jpn. **60**, 356 (1991).
[7] X. L. Wu, D. J. Pine, and P. K. Dixon, Phys. Rev. Lett. **66**, 2408 (1991).
[8] T. Hashimoto and T. Kume, J. Phys. Soc. Jpn. **61**, 1839 (1992).
[9] J. W. van Egmond, D. E. Werner, and G. Fuller, J. Chem. Phys. **96**, 7742 (1992).
[10] V. Mavrantzas and A. Beris, Phys. Rev. Lett. **69**, 273 (1992).
[11] T. Takebe and T. Hashimoto, Polymer Commun. **29**, 261 (1988); T. Takebe, F. Fujioka, R. Sawaoka, and T. Hashimoto, J. Chem. Phys. **93**, 5271 (1990); T. Hashimoto, T. Takebe, and K. Asakawa, Physica (Amsterdam) **194A**, 338 (1993).
[12] E. Mendes, Jr., P. Lindner, M. Buzier, F. Boue, and J. Bastide, Phys. Rev. Lett. **66**, 1595 (1991).
[13] R. Oeser, C. Picot, and J. Herz, in *Polymer Motion in Dense Systems*, Springer Proceedings in Physics Vol. 29 (Springer Berlin, 1988).
[14] J. Bastide, F. Boue, E. Mendes, F. Zelinski, M. Buzier, G. Beinert, R. Oeser, and C. Lartigue, in "Polymer Network 91," edited by S. I. Kuchanov and K. Dusek, VSP Utrecht, 1992 (to be published), pp. 123–149.
[15] J. Bastide, L. Leibler, and J. Prost, Macromolecules **23**, 1821 (1990).
[16] A. Onuki, J. Phys. II (France) **2**, 45 (1992).
[17] Y. Rabin and R. Bruinsma, Europhys. Lett. **20**, 79 (1992).
[18] T. Inoue, M. Moritani, T. Hashimoto, and H. Kawai, Macromolecules **4**, 500 (1971).
[19] S. Inoue, *Video Microscopy* (Plenum, New York, 1989). We made extensive use of the Image program developed by Wayne Rasband at NIH.
[20] This approach is due to Y. Rabin (private communication).
[21] F. Brochard and P. G. de Gennes, Phys. Chem. Hydrodyn. **4**, 313 (1983).
[22] M. Doi and A. Onuki, J. Phys. (Paris) **2**, 1631 (1992).

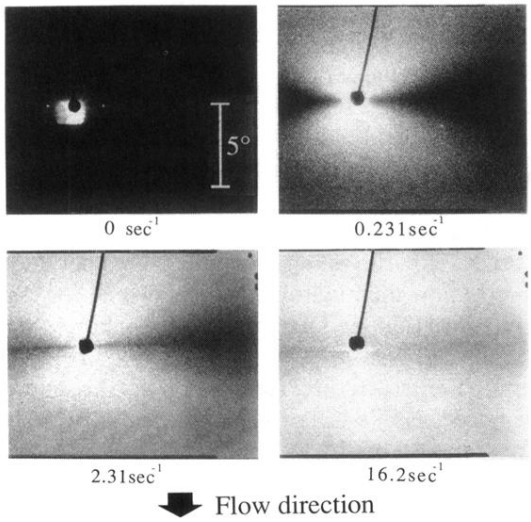

FIG. 1. SALS patterns show the appearance and development of the butterfly pattern. Photographs taken at 1/250 sec shutter speed, except for 0 sec^{-1}, taken at 1/30 sec. The halo around the beam stop at 0 sec^{-1} gives an indication of the parasitic scattering.

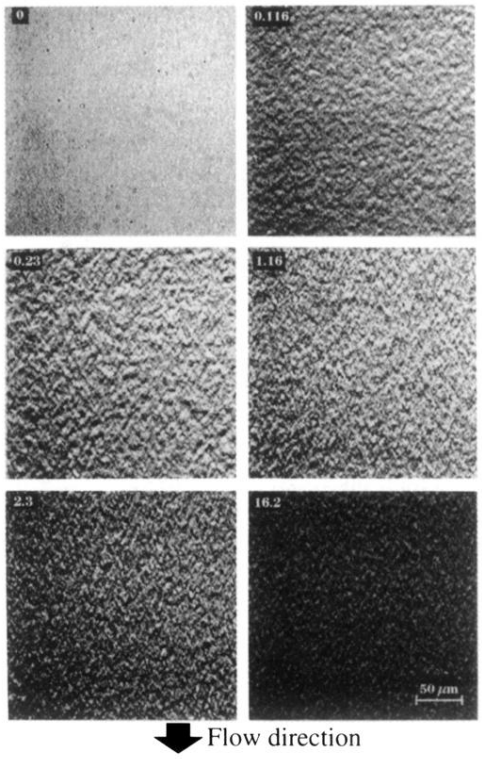

FIG. 2. Microscope visualization images of the concentration fluctuations. Numbers indicate shear rate in sec^{-1}.

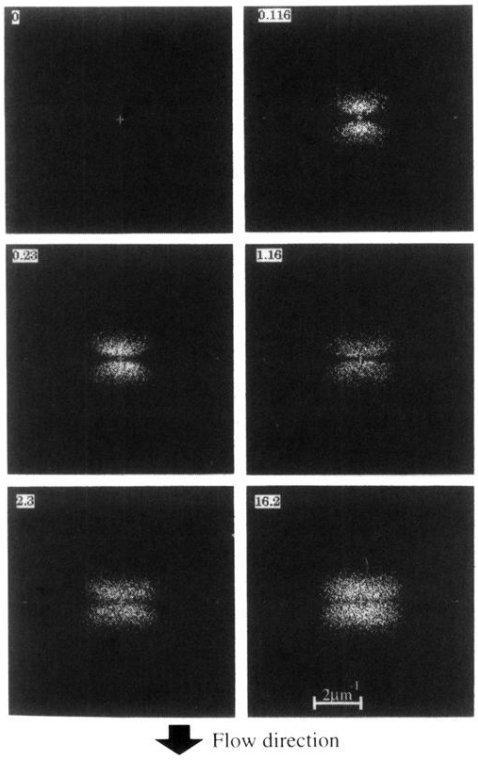

FIG. 3. FFT spectra of the images as in Fig. 2.

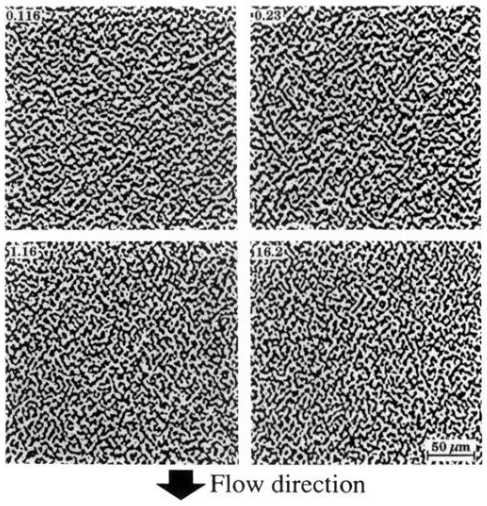

FIG. 4. Microscope images after bandpass convolution and thresholding. Numbers indicate shear rate in sec^{-1}.